INSTITUTE OF PHYSICS PUBLISHING NANOTECHNOLOGY
Nanotechnology **15** (2004) 1831–1836 PII: S0957-4484(04)83984-9

Nanocrystal formation in annealed a-$SiO_{0.17}N_{0.07}$:H films

Sandeep Kohli[1], Jeremy A Theil[2], Patricia C Dippo[3], K M Jones[3], Mowafak M Al-Jassim[3], Richard K Ahrenkiel[3], Christopher D Rithner[1] and Peter K Dorhout[1]

[1] Department of Chemistry, Colorado State University, Fort Collins, CO 80523, USA
[2] Agilent Technologies, MS 51L-GW, 5301 Stevens Creek Boulevard, Santa Clara, CA 95051, USA
[3] Measurements and Characterization Division, National Renewable Energy Laboratory, 1617 Cole Boulevard, Golden, CO 80401, USA

E-mail: skohli@lamar.colostate.edu

Received 23 July 2004, in final form 26 October 2004
Published 18 November 2004
Online at stacks.iop.org/Nano/15/1831
doi:10.1088/0957-4484/15/12/024

Abstract
Silicon nanocrystals have been fabricated by annealing amorphous hydrogenated silicon-rich oxynitride (SRON) films in vacuum for 4 h over the temperature range 850–1150 °C. X-ray photoelectron spectroscopy confirmed the composition of the film to be $SiO_{0.17}N_{0.07}$. Glancing angle x-ray diffraction results revealed consistent silicon crystallite sizes of ∼5 nm for films annealed at temperatures ⩽1050 °C, increasing to ∼12 nm for films annealed at 1150 °C. The room temperature photoluminescence spectra of the samples annealed at 850 and 950 °C comprised luminescent peaks from silicon nanocrystals and luminescence from the defects in Si–O system. However, only peaks from defects in Si–O system were present in the luminescence spectra from samples annealed at temperatures greater than 950 °C. For the samples annealed at 850 and 950 °C, the presence of strong Si–N bonds prevented the coalescence of smaller silicon crystallites into larger crystallites. Larger, non-luminescent silicon crystallites were only formed in films annealed at temperatures greater than 950 °C, where the energetics of coalescing particles overcame the strong Si–N bonding in SRON films. High-resolution transmission electron microscopy analysis confirmed the presence of silicon nanocrystallites. A proposed growth mechanism of silicon nanocrystals is discussed.

1. Introduction

Light emitting semiconductor nanocrystals of group IV materials [1–4], in particular Si [5–7], have been the subject of extensive studies due to their potential commercial applications. Although porous silicon (PS) based electroluminescent (EL) devices exhibit higher external quantum efficiency (EQE) as compared to the EL devices based on Si nanocrystals embedded in an SiO_2 matrix, the mechanical and optical instability of PS has made it difficult to incorporate it into the majority of device applications [8]. One of the major reasons for the low EQE of EL devices based on embedded silicon nanocrystals is the low volume fraction of embedded silicon nanocrystals. Attempts to increase the volume fraction of embedded silicon nanocrystals by increased silicon content yielded higher volume fractions of large non-luminescent silicon nanocrystallites.

Numerous reports have appeared in the literature investigating the nanocrystal precipitation in silicon-rich oxide (SRO) films. In some of these [9, 10] it has been reported that the presence of nitrogen played an important role in the crystallization kinetics of SRO materials. Smaller silicon crystallites were formed in SRO films containing nitrogen as compared to films without nitrogen [9]. Hence Si–O–N films are likely candidates for the fabrication of a large volume fraction of small embedded silicon nanocrystallites.

Films of Si–O–N (silicon oxynitride) exhibit a large variation in refractive index [11, 12], thus enabling the design of a large variety of waveguide structures [13]. Si–O–N films are also among the leading candidates to replace SiO_2 for sub-0.13 μm technology that requires a SiO_2 film thickness below 2 nm [11, 14].

In this paper, we report our results for the fabrication of large volume fractions of small and luminescent silicon nanocrystallites fabricated by high-temperature annealing of plasma enhanced chemical vapour deposited a-$SiO_{0.17}N_{0.07}$:H films.

2. Experimental details

Low temperature plasma enhanced chemical vapour deposition (PECVD) [15] was used to deposit 130 nm a-$SiO_{0.17}N_{0.07}$:H films on Si(100) substrates, with a 500 nm SiO_2 interlayer between the SRON film and the silicon substrate. The SiO_2 interlayer was deposited on Si wafers using PECVD [15]. The thickness of the a-$SiO_{0.17}N_{0.07}$:H layer was estimated by x-ray reflectivity (XRR) and found to be 135 ± 3 nm. For annealing purposes, the films were sealed in fused silica ampoules with a 12 mm inner diameter, and evacuated to a pressure less than 10^{-2} Pa. An annealing furnace was preheated to the targeted temperature and allowed to stabilize for 1 h. Sealed ampoules were then placed in the preheated furnace stabilized at temperatures programmed between 850 and 1150 °C for 4 h and then they were allowed to cool to the room temperature in the furnace.

Glancing angle x-ray diffraction (GAXRD) XXR, x-ray photoelectron spectroscopy (XPS), Fourier transform infrared (FTIR) spectroscopy, room temperature photoluminescence (PL) and high-resolution transmission electron microcopy (HR-TEM) were used to characterize the as-deposited and annealed films. The experimental details for GAXRD, XPS, XRR and FTIR have been published elsewhere [16–18]. Cu Kα radiation was used for the GAXRD and XRR measurements, while monochromatic Al Kα ($E = 1486.6$ eV) was employed as an x-ray source for the XPS studies. Integrated peak intensities under the O 1s, Si 2p, N 1s and C 1s XPS peaks were used for estimating the relative elemental compositions of the films. The integrated XPS peak area was normalized with respect to each core level atomic sensitivity factor [19]. GAXRD measurements were performed at an angle of incidence of 0.5°. The Warren–Averbach (WA) [20] single peak method was used to estimate the crystallite size and strain values using the Si(111) at 28.44°.[4] The single peak method was used due to the absence of higher order reflections with adequate signal to noise ratios. A standard Si sample (see footnote 4), measured under similar conditions, was used as a control as well as to estimate the strain in our samples. Winfit software was used for peak fitting and analysis [21]. The PL data were taken using an Oriel InstaSpec IV CCD and the MS-257 Imaging Spectrograph, with the InstaSpec data acquisition software. The data were corrected for system response, neutral density filters, and long pass filters. The laser used for excitation was a Kimmon IK Series 442 nm He–Cd laser at 20 mW. An interference filter was used to pass only the laser line. The HR-TEM measurements were performed using a Philips CM-30 system.

[4] JCPDS-ICDD Card No 27-1402. International Centre for Diffraction Data, Newton Square, PA.

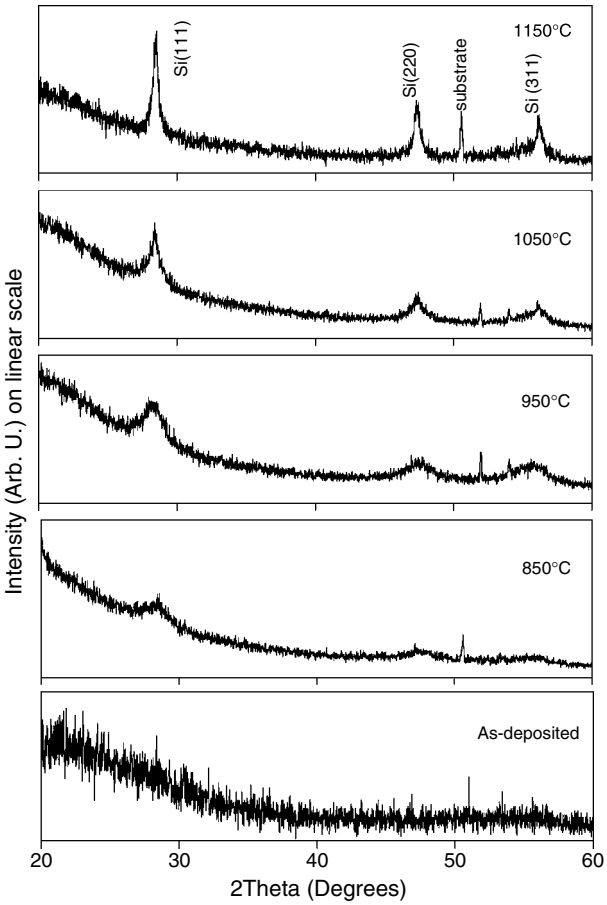

Figure 1. GAXRD spectra of as-deposited and annealed SRON film samples at an incident angle of 0.5°. The Miller indices of the reflections from the Si nanocrystals are also shown.

3. Results

As seen in figure 1, while the GAXRD pattern for the as-deposited SRON was punctuated by the absence of crystalline diffraction peaks, the silicon diffraction peaks appeared in the diffraction pattern for the samples annealed between 850 and 1150 °C. The estimated crystallite sizes were found to be 5 ± 2 nm for the samples annealed at annealing temperatures $\leqslant$1050 °C, increasing to 12 ± 1 nm for the samples annealed at 1150 °C.

The XPS survey scans for the as-deposited and annealed samples after 5 min of Ar^+ ion sputtering to expose the underlying sample surface indicated an O/Si ratio of 0.17 and an N/Si ratio of 0.07. The high-temperature annealing did not cause any changes in the O/Si and N/Si ratios.

Figure 2 shows the FTIR absorbance spectra of the as-deposited sample and the sample annealed at 850 °C. Spectra for the as-deposited sample showed the presence of hydrogen bonded to silicon (2000–2200 cm^{-1}) and Si–O stretching peaks around 1080 cm^{-1} [22, 23]. The peak for hydrogen bonded to silicon was absent in the annealed sample (850 °C) while the Si–O peaks were shifted towards higher energies. The FTIR spectra of the samples annealed at 950–1050 °C were similar

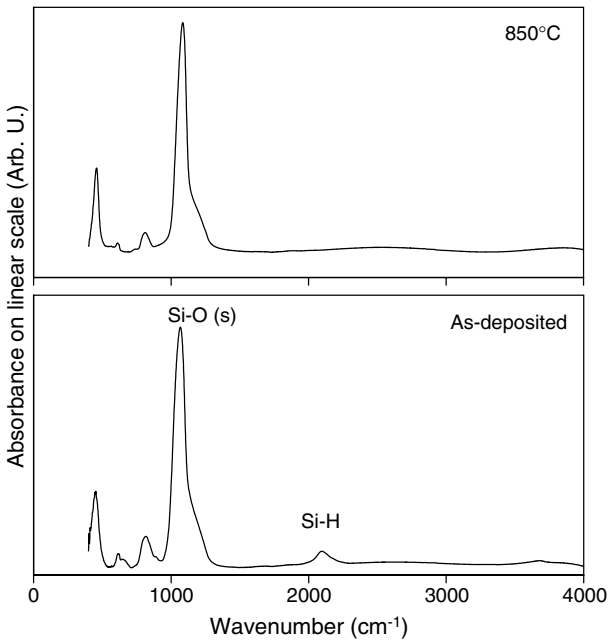

Figure 2. FTIR absorbance spectra for an as-deposited sample and a sample annealed at 850 °C.

to that of the sample annealed at 850 °C. Si–N stretching peaks in Si_3N_4 are typically found around 850 cm^{-1}, while the Si–O stretching peak in SiO_x films can shift from 1075 to 965 cm^{-1} with decreasing oxygen content [24]. It has also been observed that in the FTIR spectra of SiO_xN_y films, the dominant single phase Si–O/Si–N stretching vibration maxima varied from 850–1072 cm^{-1} for $0.26 \leqslant x \leqslant 2.0$ and $1.2 \geqslant y \geqslant 0$ [25]. Hence, the broad overlapping peaks from various nitride, suboxide and oxynitride peak components made the deconvolution of the individual peak component impractical. A broad Si–O stretching peak from the underlying 500 nm SiO_2 added to the complexity.

Room temperature PL spectra of as-deposited and annealed films are shown in figure 3. The PL spectrum of the as-deposited film showed a broad PL peak centred at 1.5 eV and a small shoulder at 1.8 eV. The film annealed at 850 °C showed broad peaks centred at 2.5, 2.0, 1.8, and 1.7 eV. The PL spectrum of the films annealed at 950 °C showed the presence of PL peaks centred at 2.5, 2.0, and 1.8 eV. However, the PL spectra of films annealed at 1050 and 1150 °C showed the presence of PL peaks at 1.9 and ∼2.5 eV. The relative intensity of the peak at 2.5 eV increased with annealing temperatures. PL peaks were not seen in the 500 nm SiO_2 layer.

Figure 4 shows representative cross-sectional HR-TEM images of the a-$SiO_{0.17}N_{0.07}$ film annealed at (a) 850 °C and (b) 1150 °C. The TEM data analysis of the sample annealed at 850 °C (figure 4(a)) indicated that the a-$SiO_{0.17}N_{0.07}$ film region was a mixed phase material containing a high volume of silicon nanocrystals. The latter exhibited a fringe contrast from (111) lattice planes in Si as opposed to the random amorphous matrix. The crystals were not uniform in shape or size but they were clearly visible by viewing the (111) lattice fringes. The nanocrystals seemed to be distributed in size between 5 and 10 nm. The sample annealed at 1150 °C is a randomly orientated nanocrystalline silicon film. This is evidenced by

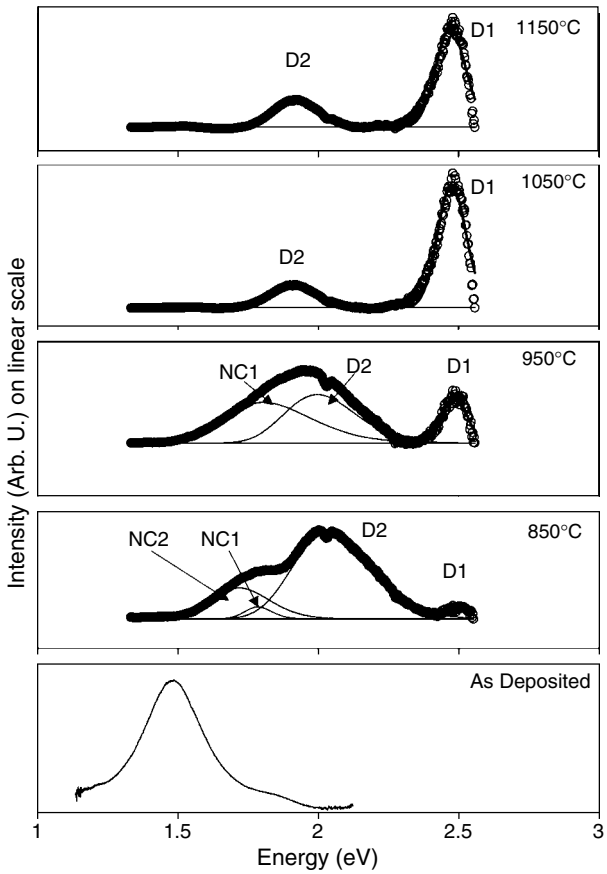

Figure 3. Fitted room temperature PL spectra of as-deposited and annealed samples. (○) experimental data; (▬) fitted curve; (——) individual peaks from a mathematical deconvolution; (- - - -) baseline. D1 and D2 are PL peaks from defects in the amorphous Si–O matrix, while NC1 and NC2 are PL peaks originating from silicon nanocrystals.

the continuous (111) lattice fringe contrast in the image. The fast Fourier transform (FFT) of a selected area from the lattice fringes (inset figure 4(b)) shows the random orientation of this film. The typical grain size was within the range 10–20 nm.

Normalized x-ray reflectivity curves over the theta-range 0.1°–1.0° for as-deposited and annealed samples are shown in figure 5. As seen in the figure, not only did the critical angle of incidence of the annealed films shift towards higher incident angle but the spacing between the fringes also increased with increasing annealing temperature, indicating the possible densification of the SRON layer. Increased amplitude of the fringes in the annealed films was due to the increased difference between the density of the SRON film and the underlying layer. The annealed films could not be simulated without the introduction of a thin (∼1.3–1.8 nm) interface layer between the 500 nm SiO_2 and SRON layer. The density of this 1–2 nm layer was estimated to be ∼2.5–2.9 g cm^{-3}. For the simulation of the x-ray reflectivity curves, the thicknesses of the underlying 500 nm SiO_2 films for as-deposited and annealed films were estimated by spectroscopic ellipsometry and fixed at appropriate values. The films annealed at higher temperatures also displayed increased surface roughness. The simulated results are shown in table 1.

Table 1. Simulated x-ray reflectivity results for as-deposited and annealed a-$SiO_{0.17}N_{0.07}$:H films.

	As-deposited		850 °C		950 °C		1050 °C		1150 °C	
Model	Thickness (nm)	Density (g cm^{-3})	Thickness (nm)	Density (g cm^{-3})	Thickness (nm)	Density (g cm^{-3})	Thickness (nm)	Density (g cm^{-3})	Thickness (nm)	Density (g cm^{-3})
Silicon oxynitride	135.4 ±2.7	2.1 ±0.1	113.3 ±2.3	2.4 ±0.1	114.1 ±2.4	2.4 ±0.1	112.6 ±2.3	2.5 ±0.1	108.2 ±2.3	2.3 ±0.1
Silicon nitride	—	—	1.8 ±0.3	2.5 ±0.2	1.6 ±0.3	2.8 ±0.3	1.6 ±0.3	2.9 ±0.3	1.3 ±0.2	2.8 ±0.3
Silicon oxide	514.2	2.3 ±0.1	514.2	2.3 ±0.1	514.2	2.3 ±0.1	514.2	2.3 ±0.1	514.2	2.3 ±0.1
Silicon substrate	—	2.32	—	2.32	—	2.32	—	2.32	—	2.32

4. Discussion

High-temperature annealing of the film structure caused silicon nanocrystal growth in the a-$SiO_{0.17}N_{0.07}$ film, without any changes in the chemical composition of the film. The average silicon crystallite size for films annealed at temperatures between 850 and 1050 °C remained constant at 5 ± 2 nm, increasing to ∼12 nm for the films annealed at 1150 °C. The absence of any bonded hydrogen (Si–H) peak in the FTIR spectra of the annealed films, within the detection limit of our FTIR spectrophotometer, was indicative of hydrogen evolution from the films as a consequence of the high-temperature annealing process. However, the changes in the Si–O stretching peak in the SRON layer were overwhelmingly masked by the broad overlapping Si–O stretching from the 500 nm SiO_2 interlayer. The shift of the Si–O stretching peak towards higher energies in the 500 nm SiO_2 layer was confirmed based on a separate set of annealing experiments performed on the SiO_2 layer. Similar results have also been reported in various reports in the literature [26, 27].

As we have shown in our recent study, the photoluminescence spectra of the as-deposited a-$SiO_{0.17}N_{0.07}$:H film was a consequence of embedded amorphous silicon particles [12]. It was also seen in this study that for samples with an O/Si ratio lower than 0.49, the O/N ratio played an important role in defining the cluster diameter; hence the PL maximum values. For all the annealed films, we observed the luminescent peaks centred at 1.95 ± 0.05 and 2.5 eV. The oxygen defect related luminescence peaks in the a-SiO_2 system are typically observed around 4.4, 3.5 and 2.4 eV [28]. The peak around 4.4 eV has been attributed to an oxygen-deficient defect, while the peaks around 3.5 and 2.4 eV are related to oxygen-excess defects [28]. The PL peak around 1.9 eV in glassy SiO_2 has also been related to an oxygen excess defect and is induced in all glassy SiO_2 exposed to various ionizing irradiations, ion implantations or mechanical stresses. Since PL peak energies at 1.9 and 2.5 eV were found to be independent of the annealing temperatures, quantum confinement effects in silicon nanocrystals were excluded from being their origin. We attribute the presence of oxygen-related defects in the Si–O system to be the origin of the 2.5 and 1.9 eV PL peaks. The films annealed at 850 and 950 °C exhibit the presence of an additional luminescence peak centred at 1.75 ± 0.05 eV. We attributed this peak to the luminescence from silicon nanocrystals. Based on a quantum mechanical model of the luminescence properties of silicon nanocrystallites, the luminescence peak at 1.75 eV corresponded to an average silicon crystallite diameter of ∼4.5 nm [29, 30]. These values are consistent with

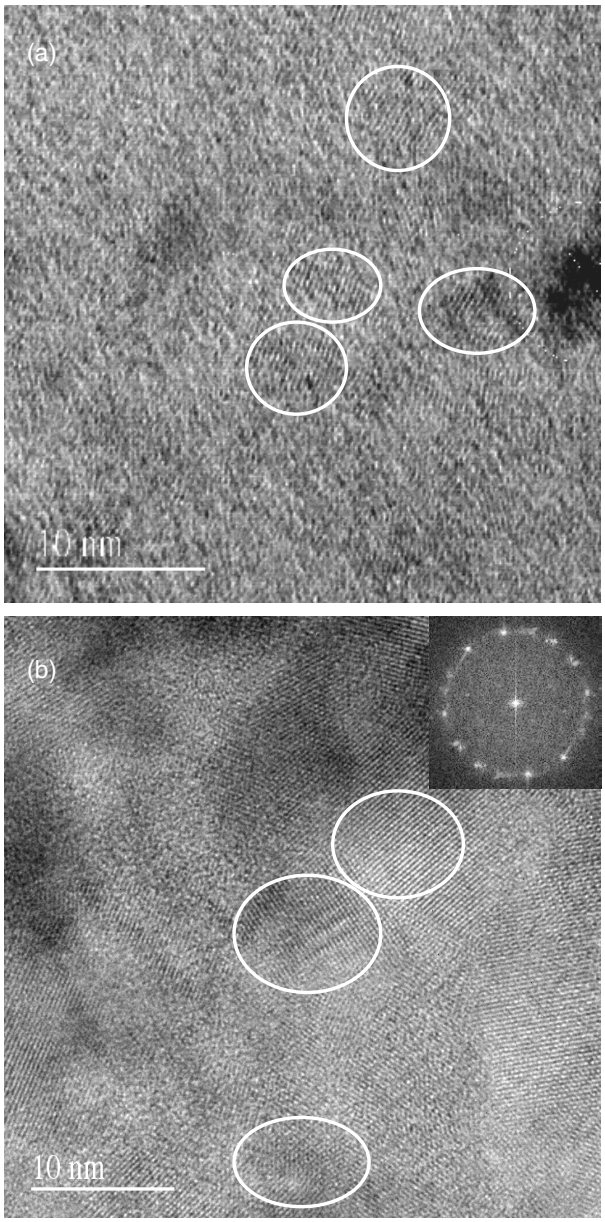

Figure 4. HR-TEM image of a sample annealed at (a) 850 °C and (b) 1150 °C.

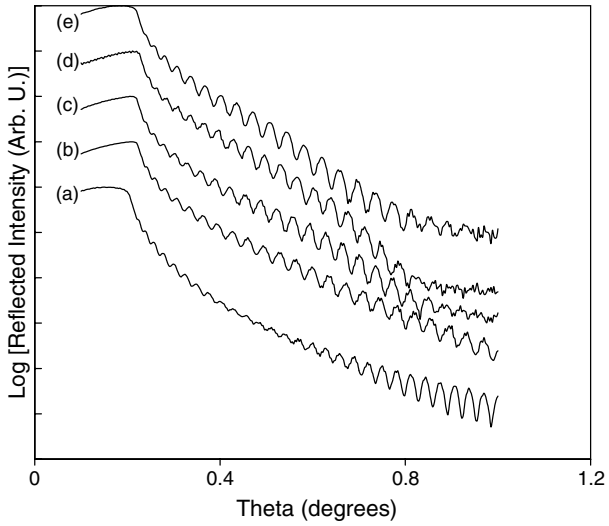

Figure 5. Normalized x-ray reflectivity for SRON films as a function of incident angle. The reflected intensity is plotted on a log axis. (a) As-deposited, (b) 850 °C, (c) 950 °C, (d) 1050 °C and (e) 1150 °C.

our GAXRD and HR-TEM results. As the annealing temperature was increased from 850 to 950 °C, the PL peak maxima did not change appreciably, possibly indicating constant crystallite sizes in the samples annealed at 850 and 950 °C. For the samples annealed at temperatures greater than 950 °C, only the luminescence from defects in the amorphous Si–O matrix was observed. It is likely that at increased annealing temperatures greater than 950 °C, a coalescence of smaller crystallites into larger, non-luminescent crystallites occurred.

The PL from oxygen-related defects was present only in annealed samples, thus indicating that these oxygen-related defects originated only during the thermal treatment in vacuum. More than 1000 studies have been reported in the literature investigating annealing characteristics of silicon-rich silicon oxide films in vacuum. It has been seen in these studies that the separation between Si and Si–O phases occurs typically at temperatures in excess of 800 °C. Higher annealing temperatures facilitate the increased phase separation between Si and SiO_2. These studies also indicate that phase separation in these silicon suboxide systems is accompanied with the stoichiometric SiO_2 formation. It is unlikely that the phase separation reaction would have contributed to the increased oxygen-related defects. However, our as-deposited films were highly silicon-rich, hydrogenated and had nitrogen as a dopant. Silicon dangling bonds were formed due to hydrogen evolution as a result of high-temperature annealing of the films. These dangling bonds were likely to be saturated with nitrogen. Similar nitrogen passivation of silicon dangling bonds has been observed in annealed nitrogen-rich silicon oxynitride films [31] and hydrogenated amorphous silicon nitride films [32]. Based on our XRR results we also found that a 1–2 nm interfacial layer with a density of ∼2.5–2.9 g cm^{-3} was also formed at the SRON–SiO_2 interlayer interface. High-density interfacial layers have also been observed in the XRR curves of nitrided SiO_2 thin film on Si wafers [33]. We also observed in these XRR results that the thickness of the film annealed at 850 °C decreased by ∼16%, and the density of the annealed film increased by ∼14%. With further annealing, no significant changes in the values of density and thickness were observed. However, no significant changes in the thickness and refractive index were observed for the 500 nm SiO_2 layer, annealed under similar conditions. Also PL peaks were not observed from the stoichiometric SiO_2 layer. It is likely that some combination of all the aforementioned changes occurring in the structure and chemistry of annealed SRON layers contributed to the presence of oxygen-related defects seen in the luminescence spectra.

The nanocrystal formation in annealed a-$SiO_{0.17}N_{0.07}$:H films can be explained in terms of hydrogen evolution and the presence of N and O impurities. Annealing the film at 850 °C led to the evolution of hydrogen from the film, which may have caused the formation of voids between silicon nanocrystals and silicon dangling bonds. These dangling bonds were likely passivated by nitrogen. Although the high-temperature annealing can also cause the coalescence of these nanocrystallites into microcrystalline silicon, the presence of N and O impurities bonded to Si prevented this. In order to achieve the coalescence of these nanocrystallites, Si–Si bonds must be formed. The bond strengths of Si–Si and Si–N bonds at 298 K are 325 ± 7 and 470 ± 15 kJ mol^{-1}, respectively [34]. Thus, the formation of Si–N bonds is energetically favoured over Si–Si bonds. Therefore, the presence of strong Si–N bonds prevented the formation of Si–Si bonds that were necessary for the coalescence of smaller Si particles to form larger crystallites. Thus, the presence of nitrogen likely enabled the formation of a large number of silicon crystallites with small crystallite size. Earlier studies of ion-implanted silicon oxide [10] and silicon-rich oxide [9] films demonstrated that the nitrogen dopant moderated the growth of silicon nanocrystals in SRON films. In both cases, the addition of nitrogen enabled the precipitation of silicon nanocrystals with reduced crystallite size as compared to undoped samples. Larger crystallites were only formed for films annealed at temperatures greater than 950 °C where the energetics of coalescing particles overcame the strong Si–N bonds.

5. Conclusions

A large volume fraction of luminescent nanocrystallites has been achieved by annealing a-$SiO_{0.17}N_{0.07}$:H films in vacuum for 4 h in the temperature range 850–950 °C. However, larger, non-luminescent crystallites were formed at annealing temperatures greater than 950 °C. The PL spectra of the samples annealed at 850 and 950 °C comprised peaks from silicon nanocrystals and luminescence from the defects in the Si–O matrix. However, only luminescence from oxygen-related defects in the Si–O matrix were present in the PL spectra of samples annealed at temperatures greater than 950 °C. HR-TEM analysis confirmed the presence of silicon nanocrystallites in films annealed between 850 and 950 °C. For the samples annealed at 850 and 950 °C, the presence of strong Si–N bonds prevented the coalescence of smaller crystallites into larger crystallites. Larger crystallites were only formed in films annealed at temperatures greater than 950 °C, where the energetics of coalescing particles overcame the strong Si–N bonding in the SRON matrix.

Acknowledgments

The authors would like to acknowledge the financial support provided by the NSF instrument Grant Nos. NSF-CHE-9808024 and NSF-DMR-0076180.

References

[1] He Z, Chen K, Xu J, Feng D, Han H and Wang Z 1998 *Proc. SPIE—Int. Soc. Opt. Eng.* **3175** 37–41
[2] Xu J, He Z H, Chen K J, Huang X F and Feng D 1999 *J. Phys.: Condens. Matter* **11** 1631–7
[3] Mikov S N, Igo A V and Gorelik V S 1999 *Phys. Solid State* **41** 1012–4
[4] Liu X, Zhang J, Yan Z, Ma S and Wang Y 2001 *Mater. Phys. Mech.* **4** 85–8
[5] Brus L 1994 *J. Phys. Chem.* **98** 3575–81
[6] Kovalev D, Heckler H, Polisski G and Koch F 1999 *Phys. Status Solidi* b **215** 871–932
[7] Cullis A G, Canham L T and Calcott P D J 1997 *J. Appl. Phys.* **82** 909–65
[8] Stewart M P and Buriak J M 2000 *Adv. Mater. (Weinheim, Fed. Repub. Ger.)* **12** 859–69
[9] Ehara T and Machida S 1999 *Thin Solid Films* **346** 275–9
[10] Kachurin G A, Yanovskaya S G, Zhuravlev K S and Ruault M O 2001 *Semiconductors* **35** 1182–6
[11] Green M L, Gusev E P, Degraeve R and Garfunkel E L 2001 *J. Appl. Phys.* **90** 2057–121
[12] Kohli S, Theil J A, Dippo P C, Ahrenkiel R K, Rithner C D and Dorhout P K 2004 *Thin Solid Films* at press (available online)
[13] Worhoff K, Hilderink L T H, Driessen A and Lambeck P V 2002 *J. Electrochem. Soc.* **149** F85–91
[14] Desbiens E, Dolbec R and El Khakani M A 2002 *J. Vac. Sci. Technol.* A **20** 1157–61
[15] Theil J A, Kooi G J and Varghese R P 2001 Chemical vapor deposition method for amorphous silicon and resulting film *European Patent Specification* 1164206
[16] Kohli S, Rithner C D and Dorhout P K 2002 *J. Appl. Phys.* **91** 1149–54
[17] Kohli S, Theil J A, Snyder R D, Rithner C D and Dorhout P K 2003 *J. Vac. Sci. Technol.* B **21** 719–28
[18] Kohli S, Theil J A, Snyder R D, Rithner C D and Dorhout P K 2003 *Proc. SPIE—Int. Soc. Opt. Eng.* **5224** 8–16
[19] Moulder J F, Stickle W F, Sobol P E, Bomben K D, Stickle W F, Sobol P E and Bomben K D 1995 *Handbook of X-Ray Photoelectron Spectroscopy—A Reference Book of Standard Spectra for Identification and Interpretation of XPS Data* (Eden Prairie, MN: Physical Electronics Inc)
[20] Warren B E 1959 *Prog. Met. Phys.* **8** 147–202
[21] Krumm S 1997 *Winfit! Package for Complete Profile-Analysis of X-Ray Reflections (profile fitting, size, strain)* Ver. 1.2
[22] Zhu M, Han Y, Wehrspohn R B, Godet C, Etemadi R and Ballutaud D 1998 *J. Appl. Phys.* **83** 5386–93
[23] Pai P G, Chao S S, Takagi Y and Lucovsky G 1986 *J. Vac. Sci. Technol.* A **4** 689–94
[24] Hinds B J, Wang F, Wolfe D M, Hinkle C L and Lucovsky G 1998 *J. Non-Cryst. Solids* **227–230** 507–12
[25] del Prado A, Martil I, Fernandez M and Gonzalez-Diaz G 1999 *Thin Solid Films* **343/344** 437–40
[26] Choi W K, Choo C K, Han K K, Chen J H, Loh F C and Tan K L 1998 *J. Appl. Phys.* **83** 2308–14
[27] Dimitrov D B, Beshkova M and Dafinova R 2000 *Vacuum* **58** 485–9
[28] Kanashima T, Okuyama M and Hamakawa Y 1996 *Japan. J. Appl. Phys.* 1 **35** 1445–9
[29] Chen X S, Zhao J J, Wang G H and Shen X C 1996 *Phys. Lett.* A **212** 285–9
[30] Trwoga P F, Kenyon A J and Pitt C W 1998 *J. Appl. Phys.* **83** 3789–94
[31] Denisse C M M, Troost K Z, Habraken F H P M, Van der Weg W F and Hendriks M 1986 *J. Appl. Phys.* **60** 2543–7
[32] Lu Z, Santos P, Stevens G, Williams M J and Lucovsky G 1995 *J. Vac. Sci. Technol.* A **13** 607–13
[33] Wang J, Lee D R, Park C, Jeong Y H, Lee K B, Park Y J, Youn S B, Park J C, Choi H M and Huh Y J 1999 *Appl. Phys. Lett.* **75** 3775–7
[34] Lide D R (ed) 2000/2001 *CRC Handbook of Chemistry and Physics* vol 81 (Boca Raton, FL: CRC Press)